A numerical method for the simulation of freight train emergency braking operations based on the UIC braked weight percentage

Rail. Eng. Science
https://doi.org/10.1007/s40534-022-00296-9

A numerical method for the simulation of freight train emergency braking operations based on the UIC braked weight percentage

N. Bosso[1] · **Matteo Magelli**[1] · **N. Zampieri**[1]

Received: 31 August 2022 / Revised: 15 December 2022 / Accepted: 16 December 2022

Abstract The present paper shows the development of a strategy for the calculation of the air brake forces of European freight trains. The model is built to upgrade the existing Politecnico di Torino longitudinal train dynamics (LTD) code LTDPoliTo, which was originally unable to account for air brake forces. The proposed model uses an empirical exponential function to calculate the air brake forces during the simulation, while the maximum normal force on the brake friction elements is calculated according to the indication of the vehicle braked weight percentage. Hence, the model does not require to simulate in detail the fluid dynamics in the brake pipe nor to precisely know the main parameters of the braking system mounted on each vehicle. The model parameters are tuned to minimize the difference between the braking distance computed by the LTDPoliTo code and the value prescribed by the UIC 544-1 leaflet in emergency braking operations. Simulations are run for different configurations of freight train compositions including a variable number of Shimmns wagons trailed by an E402B locomotive at the head of the train, as suggested in a reference literature paper. The results of the proposed method are in good agreement with the target braking distances calculated according to the international rules.

Keywords Railway brake modelling · Emergency braking · UIC braking system · Braked weight · Longitudinal train dynamics

✉ Matteo Magelli
matteo.magelli@polito.it

[1] Department of Mechanical and Aerospace Engineering, Politecnico di Torino, C.so Duca degli Abruzzi 24, 10129 Turin, Italy

1 Introduction

The calculation of the in-train forces is of great interest in braking operations, whereby large compressive forces can arise on the coupling elements, thus increasing the derailment risk. Currently, the calculation of the in-train forces is commonly carried out relying on longitudinal train dynamics (LTD) simulators [1, 2], which typically model the train consist as a system of lumped masses, corresponding to the vehicles, connected to each other by means of nonlinear elements, which feature the nonlinear impedance characteristics of the coupling elements [3–5]. Hence, common LTD simulators only model the longitudinal degree of freedom (DOF) of each vehicle in the train composition, and the effect of curves and grades is considered by adding equivalent forces applied in the longitudinal direction.

The authors' research group developed in past activities the in-house MATLAB LTDPoliTo code [6–8], which was validated on the simulation scenarios proposed in the context of the international benchmark of LTD simulators [9, 10] ("the benchmark" in the rest of the paper). However, the LTDPoliTo code in its original form does not consider the braking forces due to the air brake system, as the air brake forces were outside the scope of the benchmark and only dynamic braking forces provided by the locomotives were considered. Nonetheless, to improve the modelling capabilities of the code, a module for the computation of the air brake forces is an essential upgrade.

The recent review paper by Wu et al. [11] distinguishes three main kinds of modelling strategies for the computation of the air brake forces, namely empirical, fluid-dynamics and fluid-empirical models.

Published online: 07 March 2023

Clearly, models that simulate in detail the brake pipe require higher computational efforts despite ensuring a better accuracy, while empirical models guarantee a simpler implementation in numerical codes and allow to obtain the fastest simulation times. In fact, models that calculate the brake pipe pressure along the train, like the UIC-approved TrainDy code [12, 13], must solve the fluid-dynamics partial derivative differential equations (continuity, momentum and possibly energy balance equations), which require a high computational load and the implementation of proper methods, with the finite element and finite difference methods, together with the method of characteristics, being the most common ones according to the in-depth review by Wu et al. [11]. Therefore, fluid-dynamics and fluid-empirical models may require numerical solvers and integration time steps completely different from the ones needed for the LTD simulations, so that the development of complex parallel computing and co-simulation techniques [14, 15] may be crucial to ensure reasonable computational times. To simplify the model of the air brake pipe, a possible approach is the development of lumped models [16], in which the partial derivative differential equations are replaced by ordinary differential equations. Nonetheless, the computational effort required by the calculation of the pressure in each node of the air brake pipe can still be the bottleneck of the simulation. Moreover, for lumped models, a crucial issue is the identification of the values of the lumped parameters.

Therefore, as a big point of merit of the original LTDPoliTo code is its computational efficiency, it is the authors' belief that the best option to upgrade the code is the development of an empirical model, in which the time history of the brake block forces is calculated with a heuristic equation. Nonetheless, common empirical models may require the knowledge of several parameters of the train brake system, such as the brake cylinder diameter, the brake cylinder spring return force and the brake rigging ratios. Therefore, in this work, the authors propose a new approach for the simulation of the braking operations of freight trains equipped with the UIC brake. The main novelty of this method lies in the computation of the braking force, which is performed based on the indication of the wagon braking weight percentage, as prescribed by the UIC 544-1 leaflet [17]. In the present paper, emergency braking simulations are run to tune and validate the model, since the UIC leaflets prescribe the braking distance as a function of the braked weight for emergency braking operations in P position. Nonetheless, the proposed method can be easily extended to other braking regimes and operations, as long as a proper set of model coefficients, different from the one adopted for emergency operations, is identified.

Scholars from Politecnico di Milano (PoliMi) [16, 18] introduced a similar approach that considers the wagon deceleration as proportional to the braked weight percentage, with a proportionality term determined from numerical tests on the data given in the UIC 544-1 leaflet. Nonetheless, in the PoliMi model the brake pipe pressure is determined via a lumped model, based on the fluid-dynamics equations. On the other hand, the method proposed in the present paper relates the maximum value of the total force on all brake blocks to the wagon braked weight, but the instantaneous force is calculated in each time step with an empirical exponential function.

The paper is organized as follows. The next section describes in detail the modelling approach, and then, the results of preliminary simulations run to assess the modelling capabilities of the proposed strategy are shown. Finally, the paper is closed with conclusions and a discussion on possible future activities to improve the model.

2 Model description

The present section shows in detail the LTD model implemented in the original MATLAB LTDPoliTo code as well as the new method for the computation of the air brake forces, based on the indications of the UIC 544-1 leaflet. Moreover, in this section, focus is also given to the simulated scenario selected for the validation of the proposed approach, highlighting the main properties of the vehicles considered in the simulations.

2.1 LTD model

As most LTD simulators do, the LTDPoliTo code models the train consist only considering the longitudinal DOF of each wagon in the train consist. Hence, the LTDPoliTo code solves a system of ordinary differential equations (ODEs) in the form of Eq. (1):

$$\rho_{\text{in}} M_{\text{v}} \ddot{x} = F_{\text{c,f}} - F_{\text{c,r}} + F_{\text{t/DB}} - F_{\text{air}} - F_{\text{ord}} - F_{\text{g}} - F_{\text{crv}}, \tag{1}$$

where M_{v} is the vehicle mass; ρ_{in} is the inertia factor, accounting for the inertia of the rotating masses, which is set to 1.04 and 1.15 for wagons and locomotives, respectively; $\ddot{x}$ is the vehicle acceleration; $F_{\text{c,f}}$ and $F_{\text{c,r}}$ are the forces on the front and rear coupling elements, respectively; $F_{\text{t/DB}}$ is the force due to traction and dynamic braking, which is zero for non-powered vehicles; F_{ord} is the resistant force due to rolling resistances and aerodynamic drag; F_{g} is the force due to track grade; F_{crv} is the curving resistance; and finally F_{air} is the air brake force. Please note that the in-train force on the front coupler of the leading

vehicle and the force of the rear coupler on the tail end wagon are zero.

Obviously, since the goal of the present paper is the definition of a simplified method for the calculation of the air brake forces, the simulated scenarios only include straight level sections, hence the contributions due to gravity and curves are zero on all vehicles. At the same time, forces due to traction/dynamic braking are zero on powered vehicles, as the simulations are only limited to braking operations in which the braking effort is provided by the air brake system, and no contribution is given by dynamic braking.

Several expressions are used in the literature for the calculation of the ordinary resistant forces [19]. In the present work, the expression suggested in the international benchmark of LTD simulators is adopted, since it features an explicit dependency on the number of vehicle axles and on the axle load, see Eq. (2):

$$F_{\mathrm{ord}} = \frac{M_{\mathrm{v}}}{1000}\left(2.943 + \frac{89.2}{Q_{\mathrm{ax}}} + 0.0306V + \frac{0.122V^2}{Q_{\mathrm{ax}}N_{\mathrm{ax}}}\right), \tag{2}$$

where Q_{ax} is the axle load (t), V is the vehicle speed (km/h) and N_{ax} is the number of axles.

In the LTDPoliTo code, the forces on the coupling elements are computed from fixed look-up tables (LUTs), which store the loading and unloading curves of the impedance characteristic as a function of the coupler deflection. A big advantage of the LUT approach, compared to other strategies witnessed in the literature [5], is that it can be easily adapted to manage both the European buffer–hook system and the automatic coupler adopted in the rest of the world. To avoid numerical instabilities, a smoothing transition is prescribed between the two curves when the deflection speed is below a fixed threshold, as suggested by Zhang et al. [20], see Eq. (3):

$$F_{\mathrm{c}} = \begin{cases} F_{\mathrm{L}}(\Delta x), & |\Delta\dot{x}| > v_{\mathrm{th}} \quad \text{(Loading)} \\ F_{\mathrm{U}}(\Delta x), & |\Delta\dot{x}| > v_{\mathrm{th}} \quad \text{(Unloading)} \\ \dfrac{F_{\mathrm{L}}(\Delta x) + F_{\mathrm{U}}(\Delta x)}{2} + \dfrac{|F_{\mathrm{L}}(\Delta x) - F_{\mathrm{U}}(\Delta x)|}{2} \cdot \dfrac{\Delta\dot{x}}{v_{\mathrm{th}}}, & |\Delta\dot{x}| \le v_{\mathrm{th}} \end{cases}, \tag{3}$$

where F_{c} is the force on the coupling element, Δx is the deflection of the coupling element, $\Delta\dot{x}$ is the deflection speed of the coupling element, F_{L} and F_{U} are the forces corresponding to the loading and unloading curves, respectively, and v_{th} is the threshold speed.

Finally, the air brake forces are computed according to the new proposed method, which is described in detail in the following subsection.

2.2 Computation of the air brake forces

The proposed model for the computation of the air brake forces on European freight trains is based on the prescriptions of the UIC 544-1 leaflet, which is the UIC leaflet for the computation of the braking power of railway vehicles. In fact, the leaflet provides an expression that relates the braked weight of railway wagons to the sum of all brake block forces, see Eq. (4):

$$B = \frac{k \cdot \sum F_{\mathrm{dyn}}}{g}, \tag{4}$$

where the same symbols as in the UIC 544-1 leaflet are used: B is the wagon braked weight (t), $\sum F_{\mathrm{dyn}}$ is the sum of all brake block forces (kN), g is gravity and finally k is a parameter which depends on the block configuration and on the force on each block F_{dyn}, see Fig. 1, which also highlights the dependency of the braked weight on the brake block force for both Bgu and Bg configurations. Equation (1) is valid only for wagons with maximum speed below 120 km/h and maximum axle load of 22.5 t, equipped with brake shoes made of P10 cast iron and featuring a wheel diameter in the range 920–1000 mm.

According to the UIC 544-1 leaflet, the expression stated by Eq. (4) shall be used to estimate the braked weight of railway wagons once the sum of all brake block forces is calculated, starting from the knowledge of the main air brake system parameters. Conversely, the idea of the proposed method is to use Eq. (4) to compute the sum of all brake block forces starting from the knowledge of the braked weight. Clearly, as the k factor is a nonlinear function of the brake block force, a closed-form solution is impossible, and an iterative scheme is needed.

The force computed in this way can be considered as the maximum brake block force applied during emergency braking operations, which corresponds to the maximum applied brake cylinder pressure. Nonetheless, when a braking operation is started, the pressure clearly does not immediately reach its maximum value and also delays

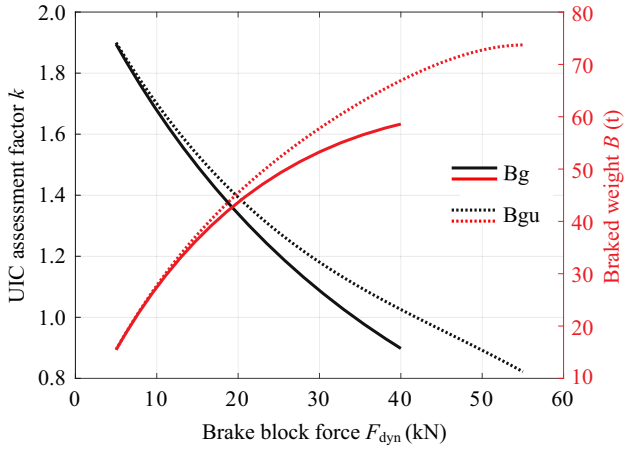

Fig. 1 k parameter (black) and braked weight (red) for Bg and Bgu block configurations as a function of the force on the brake block

along the train length exist. Therefore, to account for such delays, an empirical exponential function is introduced, see Eq. (5):

$$F_{B,tot}(t) = 1000 \sum F_{dyn} \cdot \left[1 - e^{-\frac{(t - t_{app} - t_{del})}{\tau}}\right] H(t - t_{app} - t_{del}), \tag{5}$$

where $F_{B,tot}$ is the total force on all brake blocks (N), t is time, t_{app} accounts for the delay between the beginning of the braking operation and the time instant in which the pressure in the brake cylinder starts to increase, t_{del} accounts for the delay between the leading locomotive and the other wagons, τ is the model time constant, which modifies the gradient of the force rise, and finally H is step function which is zero when its argument is negative, and otherwise it returns 1. Figure 2 qualitatively shows the evolution of the total brake block force on the head wagon and on a remote wagon, highlighting the time delays t_{app} and t_{del} introduced in Eq. (5). Please note that the term "remote" wagon refers to any wagon in the train composition behind the head wagon. Clearly, as the distance of the considered remote wagon from the train head increases, the time delay t_{del} increases, too.

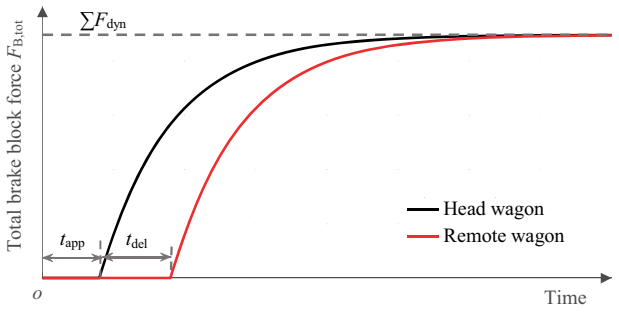

Fig. 2 Exponential heuristic function for the calculation of the brake block forces

The delay on the jth vehicle can be related to the propagation speed of the pressure drop wave in the brake pipe v_{air}, see Eq. (6):

$$t_{del} = \frac{x_N - x_j}{v_{air}}, \tag{6}$$

where x_N is the position of the leading locomotive and x_j is the position of the jth vehicle.

On the other hand, the model time constant τ can be related to the brake cylinder filling time t_{fill}, which is prescribed by the UIC 540 leaflet [21] for brake positions P and G, see Eq. (7):

$$\tau = \frac{t_{fill}}{\ln 20}. \tag{7}$$

Once the total brake block force $F_{B,tot}$ is calculated, the air brake force F_{air} can be computed according to Eq. (8):

$$F_{air} = \mu_B F_{B,tot}, \tag{8}$$

where μ_B is the brake shoe friction coefficient. For cast-iron shoes, the friction coefficient can be calculated according to the Karwatzki's equation as a function of the force on each brake block F_{dyn} (kN) and of the running speed V (km/h):

$$\mu_B = 0.6 \times \frac{V + 100}{5V + 100} \times \frac{16/gF_{dyn} + 100}{80/gF_{dyn} + 100}. \tag{9}$$

Of course, this strategy for the calculation of the air brake forces relies on the assumption that a good adhesion level is ensured at the wheel–rail interface, as most LTD simulators are not able to consider degraded adhesion conditions [22].

In conclusion, the proposed model allows to compute the air brake force on freight wagons starting from the indication of the braked weight of the wagon, with no need for a detailed knowledge of the air brake system. The model requires the tuning of three main parameters, namely the depression wave propagation speed, the delay due to the application of brake pressure and the brake cylinder filling time.

Nonetheless, the main drawback of the proposed method is that the strategy for the computation of the brake block forces, based on Eq. (4), is only valid for freight wagons. To solve this issue, in the present paper Eq. (4) is extended to locomotives by identifying a constant value of the k parameter, which is searched via an optimization algorithm, as shown in the following lines. This approach is similar to the one adopted by Di Gialleonardo et al. [18], who searched for a constant coefficient to relate the braked weight percentage to the braking deceleration of freight wagons.

Since locomotives are commonly equipped with brake discs, which feature a more stable behaviour of the friction coefficient, the friction coefficient is assumed as constant

during the whole braking operation. Hence, once the sum of the normal forces acting on the discs $F_{B,tot}$ is obtained, the braking force F_{air} on the locomotive is calculated according to Eq. (10):

$$F_{air} = \mu_D \frac{d_D}{d_w} F_{B,tot} = \mu_{eff} F_{B,tot}. \quad (10)$$

where μ_D is the brake disc friction coefficient, d_D is the brake disc effective diameter, d_w is the wheel diameter and finally μ_{eff} is the effective friction coefficient which accounts for the ratio between the brake disc effective diameter and the wheel diameter. The values of μ_{eff} and of the k parameter for locomotives can be obtained by minimizing the error between the braking distance prescribed by the UIC 544-1 leaflet for isolated locomotives and the braking distance calculated with a numerical integration for different values of the initial speed. Please note that the proposed model, based on the empirical exponential expression given in Eq. (5), is developed for freight train configurations in which the brake pipe is discharged from the head locomotive and no radio signal is sent to remote locomotives to activate the braking operation from several vehicles. In fact, most European freight train configurations perform the brake discharge only at the head locomotive. To account for different train configurations, in which the brake pipe is discharged from several vehicles along the train composition, a different heuristic expression should be identified, accounting for the more complex fluid-dynamic behaviour generated in such configurations.

In the next subsection, the simulation scenarios and the main characteristics of the train compositions and vehicles considered to tune and validate the model are described in detail.

2.3 Case study

The method for the calculation of the air brake forces described in the previous sections is validated in the present paper in emergency braking operations, considering the train compositions suggested by Pugi et al. [23]. The model validation is performed with respect to the braking distances prescribed by the UIC 544-1 leaflet when available and against the results given in Ref. [23] for all other cases. The proposed approach can be also adapted to consider non-emergency braking operations, as long as a dedicated tuning of the model parameters for this kind of operations is carried out. However, in this paper, the model is validated in emergency braking operations, for which the UIC 544-1 leaflet provides the values of the braking distances as a function of the braked weight. Future work will deal with an extension of the model to consider service braking operations.

The train compositions provided in Ref. [23] and considered in this paper always include a variable number of Shimmns wagons trailed by a E402B locomotive. Currently, the E402B locomotive is only used in passenger trains; however, in past years it was also adopted in freight trains travelling between Italy and France. Therefore, in the present paper the E402B locomotive is considered since the main vehicle data are provided in Ref. [23].

As reported in Ref. [23], the Shimmns wagon has a maximum axle load of 22.5 t and it is provided with a double-stage empty-loaded device which adjusts the braking force according to the wagon loading condition. Therefore, the braked weight percentage is not constant, and it features a sharp transition near the changeover weight of 48 t, due to the intervention of the empty-loaded device, see Fig. 3. On the other hand, the E402B locomotive features a weight on rails of 89 t and a braked weight of 79 t, which corresponds to a braked weight percentage equal to approximately 90%.

The length of each Shimmns wagon is equal to 12.64 m, while the length of the E402B locomotive is equal to 19.42 m. All wagons are connected by means of the typical buffer–hook system adopted on European vehicles, with buffers having an initial length of 620 mm and a maximum stroke of 105 mm. The library of the LTDPoliTo code includes an experimental LUT for the buffer–hook system, but in this work, a new LUT is built starting from the buffer and hook mechanical impedance characteristics plotted in Ref. [23], see Fig. 4, in which negative forces and deflections correspond to compressive states (buff conditions), while positive forces and deflections are relative to tensile states (draft conditions).

3 Results

The present section shows the results of the validation of the proposed model for the calculation of the braking distance of freight trains in emergency braking operations.

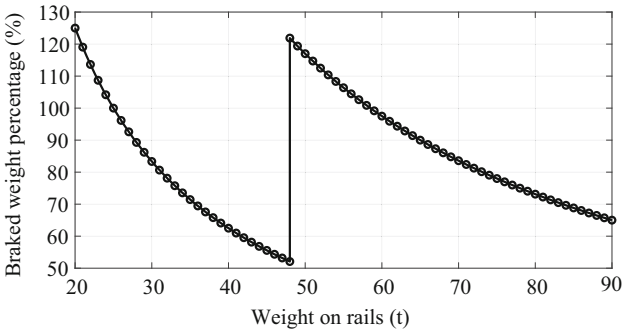

Fig. 3 Braked weight percentage of the Shimmns wagon as a function of the wagon weight on rails

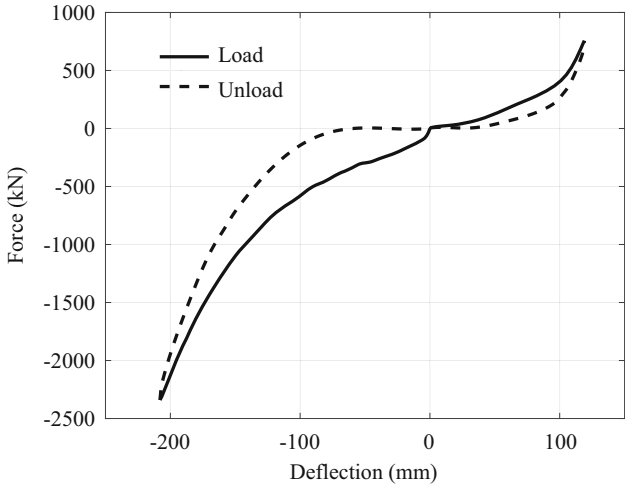

Fig. 4 Impedance characteristics of the coupling system considered in the work by Pugi et al. [23]

The main model parameters are tuned on the simulation scenarios presented in the research paper by Pugi et al. [23] in which all vehicles are braked in position P. Ref. [23] shows the results for different train compositions and for two values of starting speed, i.e., 100 km/h and 50 km/h. The model adopted in Ref. [23] is a fluid-dynamics model that computes the pressure along the brake pipe and the pressure in the brake cylinders according to the well-known fluid-dynamics equations [24]. On the other hand, with the method proposed in the present paper and described in the previous section, the brake block force on the Shimmns wagons is calculated by applying Eq. (4) starting from the knowledge of the braked weight, while the total normal force on the brake pads on the head locomotive is obtained by still applying Eq. (4) after identifying the constant value of the k factor for locomotives and the effective friction coefficient for brake discs via an optimization scheme. Please note that for the E402B locomotive, the value of the sum of the air brake forces calculated according to the simplified strategy proposed in the paper is close to the actual value that can be obtained starting from the main parameters of the air brake system.

Since different train configurations are considered in the paper, the braked weight percentage of the train λ_{train} is recalculated in each simulation scenario according to Eq. (11):

$$\lambda_{\text{train}} = k_{\text{UIC}} \frac{\sum B_{\text{f}}}{\sum Q_{\text{v}}} \times 100, \tag{11}$$

where $\sum B_{\text{f}}$ is the sum of the braked weight of all wagons on which a braking effort is applied, $\sum Q_{\text{v}}$ is the sum of the weight on rails of all wagons in the train and finally k_{UIC} is a correction factor which is equal to 1 when the train length is below 500 m, while it is less than 1 for train lengths above 500 m, as prescribed by the UIC 544-1 leaflet.

In all simulations presented in the paper, the ODE system described by Eq. (1) is solved with the LTDPoliTo code by means of the ODE15s numerical integration scheme for stiff systems directly available in MATLAB, with specification of the Jacobian sparsity pattern and a sampling time of 5 ms. The relative and absolute tolerances of the solver are set to 1×10^{-7} and 1×10^{-8}, respectively, while the threshold speed value for the management of the transition between the loading and unloading curves describing the hysteretic behaviour of the coupling elements, see Eq. (3), is set to 0.1 mm/s.

Tables 1 and 2 show the results of the simulations run for the model parameter tuning, for initial speeds of 100 km/h and 50 km/h, respectively, highlighting the train composition, the braked weight of the train λ_{train}, computed according to Eq. (11), the braking distance according to the UIC 544-1 leaflet, the braking distance calculated by Pugi et al. using the fluid-dynamics model of Università di Firenze (UniFi) and the braking distance calculated by the Politecnico di Torino (PoliTo) research group using the LTDPoliTo code. The last column of Tables 1 and 2 gives the results in terms of the maximum in-train force in draft and buff conditions, also specifying the coupler on which the maximum force is recorded during the simulation. Couplers are numbered in ascending order starting from the first coupler behind the leading locomotive. The train composition is defined for each simulation with a string in the form of "*N* w (*W* t)", where *N* indicates the number of wagons in the train composition and *W* is the weight on rails of the wagons (all wagons in the train composition have the same axle load). As previously mentioned, all train compositions include an E402B locomotive at the head of the train, and the empty-loaded device is in "loaded" positions on all wagons. Of course, for the simulations run with an initial speed of 50 km/h, the braking distance according to the UIC leaflet is not available, and the corresponding column is filled with "NA".

Figure 5 plots the normalized braking distance calculated in each simulation run to in this initial stage of the model validation. The normalized braking distance is obtained by setting in each simulation scenario the UIC braking distance to 1. In simulations 7–12, run with initial speed of 50 km/h, the UIC braking distance is not available, so the distance obtained by the UniFi researchers is used as reference and set to 1.

As noticeable from Table 1 and Fig. 5, the results of the LTDPoliTo code are closer to the braking distance prescribed by the UIC 544-1 leaflet rather than to the outputs of the fluid-dynamics model adopted in Ref. [23]. In fact, during the validation process, the model parameters were tuned to ensure braking distances as close as possible to the UIC prescribed values. Table 3 presents the model parameters identified in the model tuning process via a

Table 1 Validation results for initial speed of 100 km/h

Simulation No.	Train composition	Train braked weight λ_{train} (%)	Braking distance (m)			F_{max} (kN)@Coupler position	
			UIC	Pugi	LTDPoliTo	Draft	Buff
1	10 w (80 t)	74.8	732.3	617	698.5	85@1	50@7
2	16 w (50 t)	114.3	497.6	437	484.4	167@1	91@11
3	15 w (80 t)	74.3	736.9	625	701.7	89@1	84@10
4	24 w (50 t)	117.4	494.2	449	485.4	171@1	143@15
5	20 w (80 t)	74.0	739.3	635	705.3	90@1	114@13
6	32 w (50 t)	115.6	492.5	465	489.1	171@1	205@21

Table 2 Validation results for initial speed of 50 km/h

Simulation No.	Train composition	Train braked weight λ_{train} (%)	Braking distance (m)			F_{max} (kN)@Coupler position	
			UIC	Pugi	LTDPoliTo	Draft	Buff
7	10 w (80 t)	74.8	NA	136	162.0	86@1	59@7
8	16 w (50 t)	114.3	NA	100	119.0	167@1	104@11
9	15 w (80 t)	74.3	NA	138	163.0	88@1	98@10
10	24 w (50 t)	117.4	NA	106	121.2	168@1	171@15
11	20 w (80 t)	74.0	NA	143	164.5	91@1	136@13
12	32 w (50 t)	115.6	NA	115	124.0	195@5	252@22

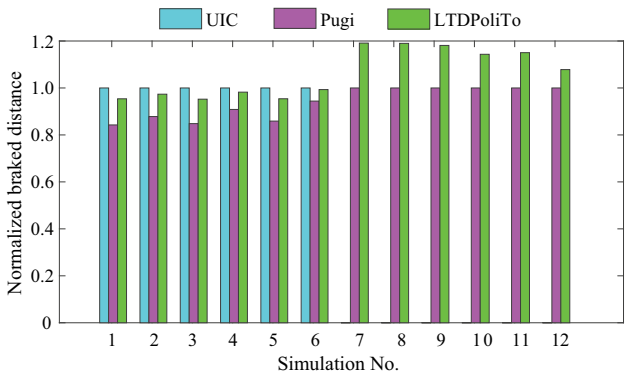

Fig. 5 Results of the model validation

trial-and-error procedure. Table 1 and Fig. 5 also highlight that the braking distance predicted by the UniFi fluid-dynamics model is always far below the braking distance prescribed by the UIC 544-1 leaflet for the corresponding braked weight percentage. Therefore, this also explains why in simulation scenarios 7–12, the braking distance predicted by the LTDPoliTo code is approximately 20% higher compared to UniFi values, see Table 2 and Fig. 5. Nonetheless, the 20% relative error is mainly due to the low values of braking distance, since the initial speed is 50 km/h and hence a small difference in the braking distance can lead to large relative errors. On the other hand, in the simulations run from an initial speed of 100 km/h, the maximum relative error between the UIC braking distance and the one computed by the LTDPoliTo code is below 5%.

Focusing on the maximum in-train forces given in Tables 1 and 2, the maximum draft force is always recorded at the head of the train composition, while the maximum buff force is obtained slightly behind the middle of the train composition, due to the propagation delay of the brake pipe pressure drop along the train. Figure 6 shows the distribution of the maximum in-train force on each coupling element from the head to the tail of the train for both buff and draft conditions, considering simulation scenario No. 6. Similar trends are obtained for all other simulation scenarios and hence they are not displayed in the paper.

Table 3 Model parameters identified via the trial-and-error procedure

Symbol	Description	Value
t_{app}	Delay between braking command and braking pressure rise in brake cylinders	1 s
v_{air}	Speed of pressure wave	200 m/s
t_{fill}	Brake cylinder filling time	5 s
k_{loco}	k factor of Eq. (5) for head E402B locomotive	3.54
μ_{eff}	Brake disc effective friction coefficient (for head locomotive)	0.264

Tensile forces are generated on the coupling connection systems because of the differences in the braked power of the E402B locomotive and of the Shimmns wagons. Moreover, the air brake force which eventually causes the deceleration of the vehicles is the product of the pressing force on the friction elements and the friction coefficient, see Eqs. (8) and (10). For the disc braked locomotive, the friction coefficient is approximately constant, while for the tread braked wagons equipped with cast-iron shoes, the friction coefficient is calculated according to the Karwatzki's expression, see Eq. (9), which predicts larger values of the friction coefficient at lower speed. Therefore, as the emergency braking operation goes on and speed is reduced, the air brake force on the tread braked wagons increases even after the maximum brake cylinder pressure is achieved on the vehicle. This phenomenon is confirmed by Fig. 7, which plots the value of the total air brake force and of the total force on all brake blocks on the head and tail wagons for simulation scenario No.6. Figure 7 highlights that in the initial stages of the simulations, the pressing force on the brake blocks of the wagons is different due to delays related to the limited propagation speed of the pressure drop along the train length. Once the total pressing force is saturated on the wagons, the air brake forces have similar values on all wagons, because due to the large stiffness of the coupling systems, all wagons in the train composition run at a similar speed. Finally, a further comparison between Tables 1 and 2 points out that when the initial speed is 50 km/h, the maximum buff in-train forces increase with respect to the values corresponding to the simulations launched with initial braking speed of 100 km/h. This is once again due to the behaviour of the friction coefficient at the wheel–shoe interface, which increases when the speed is lower.

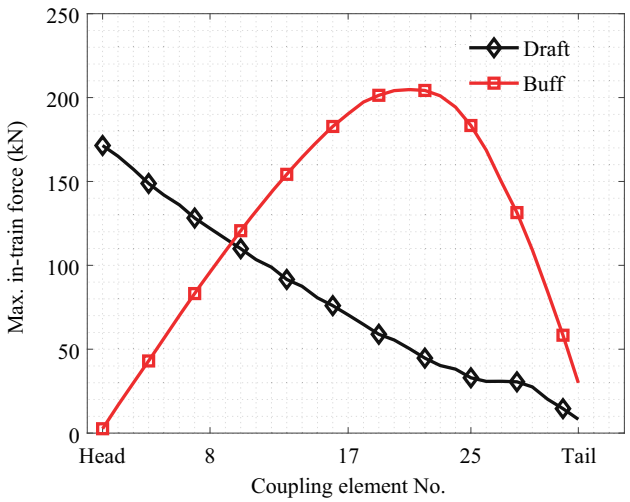

Fig. 6 Maximum in-train forces in buff and draft conditions (simulation scenario No. 6)

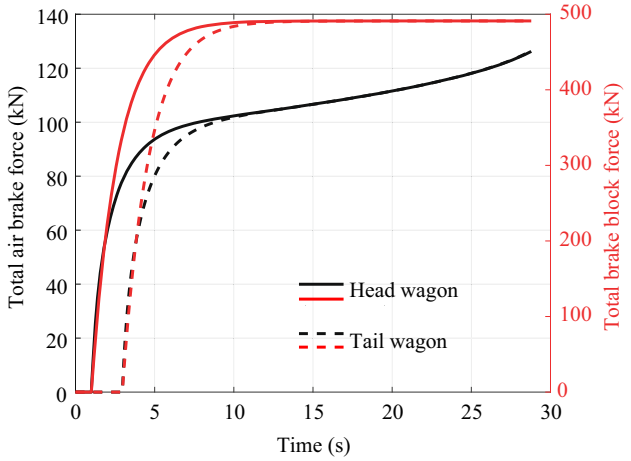

Fig. 7 Air brake force and total force on brake blocks for head and tail wagons (simulation scenario No. 6)

Since the proposed method based on Eq. (4) can be adapted for wagon speeds up to 120 km/h, simulations were run with an initial speed of 120 km/h for the same train compositions as in the previous tests summarized in Tables 1 and 2 to further validate the model. Table 4 shows the braking distances calculated with the LTDPoliTo code and the corresponding value prescribed by the UIC 544-1 leaflet. A good agreement can be observed between the two values of braking distance, with a maximum relative error of 2.93%; hence, the proposed model gives results in good agreement with the UIC prescribed braking distances even in simulation scenarios different from the ones considered to tune the main model parameters. Therefore, the proposed method ensures a good reliability in the computation of the braking distances of European freight trains. A big advantage of the proposed approach, which is also the main novelty introduced in the paper, is that the pressing forces on the brake friction elements are estimated as a function of the brake weight only, with no need for a computationally expensive fluid-dynamics model for the computation of the pressure along the brake pipe.

Focusing on the last column of Table 4, which provides the results in terms of maximum in-train forces, a comparison with Tables 1 and 2 shows again that when the initial braking speed is higher, the maximum in-train forces tend to decrease, due to the frictional characteristics of cast-iron shoes.

4 Conclusions

The main goal of the present paper is to prove the feasibility of applying a new method for the computation of the air brake forces in the simulation of braking operations of freight trains based on the prescriptions of the UIC 544-1

Table 4 Braking distances for initial speed equal to 120 km/h

Train composition	Train braked weight λ_{train} (%)	Braking distance (m)		F_{max} (kN)@Coupler position	
		UIC	LTDPoliTo	Draft	Buff
10 w (80 t)	74.8	1060.4	1033.3	85@1	48@7
16 w (50 t)	114.3	727.8	709.9	166@1	88@11
15 w (80 t)	74.3	1070.0	1038.7	89@1	81@10
24 w (50 t)	117.4	723.0	710.0	172@1	138@16
20 w (80 t)	74.0	1070.3	1044.0	90@1	110@13
32 w (50 t)	115.6	720.5	713.8	174@5	197@20

leaflet. The proposed model is tuned and validated in emergency braking operations, with the aim to minimize the difference between the simulated braking distance and the value prescribed by the UIC544-1 leaflet. In fact, the UIC 544-1 leaflet prescribes the braking distance values in emergency braking operations for vehicles braked in P position. The simulation scenarios for model tuning are extracted from a reference paper by UniFi researchers, in which a variable number of Shimmns wagons trailed by a head E402B locomotive is considered.

Nonetheless, the proposed modelling approach, which relies on an empirical function for the calculation of the air brake forces, can be easily extended to consider braking operations of European freight trains in G positions, provided that a new set of model coefficients is identified to account for the different brake cylinder filling times and delays along the train length compared to the P position.

The main outcomes of the activity shown in the paper are given in the following numbered list.

1. On the simulations run to tune the model parameters, the maximum error between the braking distance calculated by the LTDPoliTo code and the value prescribed by the UIC 544-1 leaflet is below 5%, which ensures a good accuracy of the model. After tuning the model parameters, in simulations of braking operations from an initial speed of 120 km/h, the maximum error between the UIC 544-1 and simulated braking distances is approximately equal to 2.93%.
2. When the initial speed of the train is equal to 50 km/h, the LTDPoliTo code predicts approximately 20% longer braking distances compared to the UniFi model. In fact, the LTDPoliTo model is tuned against the braking distances prescribed by the UIC 544-1 leaflet, but the UniFi model always tends to calculate larger values of the braking distance with respect to the ones specified by the UIC 544-1 leaflet.
3. Since the friction coefficient at the wheel–shoe interface in tread braked wagons is not constant and it increases at lower speeds, the total air brake force on wagons increases as the braking operations are continued, even if the total force on all brake blocks is constant.
4. Due to the different frictional behaviour of the wheel–shoe and pad–disc pairs, and due to the differences in the braked weight of wagons and head locomotive, tensile in-train forces can be generated along the train, and the magnitude of such forces decreases from the train head to the train tail end.
5. The maximum in-train force in draft conditions is always located at the head of the train, while the maximum in-train force for buff conditions is obtained in the rear part of the train composition, because of the delays in the transmission of the pneumatic signal from the head locomotive to all trailed wagons.
6. The proposed method can be considered as a reliable strategy for the computation of the air brake forces in emergency braking operations, since it predicts braking distances close to the values prescribed by the international rules as a function of the train braked weight percentage.
7. Compared to other empirical models, the biggest point of merit of the proposed strategy is that it does not require to know in detail the key parameters of the air brake system of all vehicles in the train composition, as block configuration and braked weight are the only model inputs for the calculation of the brake block forces.

Acknowledgements We thank Prof. Luciano Cantone, from Università di Roma Tor Vergata, for sharing essential information on the E402B locomotive air brake system.

References

1. Wu Q, Spiryagin M, Cole C (2016) Longitudinal train dynamics: an overview. Veh Syst Dyn 54(12):1688–1714
2. Cole C (2020) Longitudinal train dynamics and vehicle stability in train operations. In: Iwnicki S, Spiryagin M, Cole C, McSweeney T (eds) Handbook of railway vehicle dynamics. CRC Press, Boca Raton, pp 457–519
3. Cole C (1998) Improvements to wagon connection modelling for longitudinal train simulation. Presented at CORE 1998: engineering innovation for a competitive edge: conference on railway engineering, Yeppoon, Queensland, Australia
4. Massa A, Stronati L, Aboubakr AK, Shabana AA, Bosso N (2012) Numerical study of the noninertial systems: application to train coupler systems. Nonlinear Dyn 68(1):215–233
5. Wu Q, Cole C, Luo S, Spiryagin M (2014) A review of dynamics modelling of friction draft gear. Veh Syst Dyn 52(6):733–758
6. Bosso N, Magelli M, Zampieri N (2020) Long train dynamic simulation by means of a new in-house code. WIT Trans Built Environ 199:249–259
7. Bosso N, Magelli M, Zampieri N (2020) Development and validation of a new code for longitudinal train dynamics simulation. Proc Inst Mech Eng Part F J Rail Rapid Transit 235(3):286–299
8. Bosso N, Magelli M, Zampieri N (2021) Validation of a new longitudinal train dynamics code for time domain simulations and modal analyses. Int J Transp Dev Integr 5(1):41–56
9. Spiryagin M, Wu Q, Cole C (2017) International benchmarking of longitudinal train dynamics simulators: benchmarking questions. Veh Syst Dyn 55(4):450–463
10. Wu Q, Spiryagin M, Cole C, Chang C, Guo G, Sakalo A et al (2018) International benchmarking of longitudinal train dynamics simulators: results. Veh Syst Dyn 56(3):343–365
11. Wu Q, Cole C, Spiryagin M et al (2023) Freight train air brake models. Int J Rail Transp 11(1):1–49
12. Cantone L, Crescentini E, Verzicco R, Vullo V (2009) A numerical model for the analysis of unsteady train braking and releasing manoeuvres. Proc Inst Mech Eng Part F J Rail Rapid Transit 223(3):305–317
13. Cantone L (2010) TrainDy: the new union internationale des chemins de fer software for freight train interoperability. Proc Inst Mech Eng Part F J Rail Rapid Transit 225(1):57–70
14. Wu Q, Cole C (2015) Computing schemes for longitudinal train dynamics: sequential, parallel and hybrid. J Comput Nonlinear Dyn 10(6):064502
15. Wu Q, Cole C, Spiryagin M, Wang Y, Ma W, Wei C (2017) Railway air brake model and parallel computing scheme. J Comput Nonlinear Dyn 12(5):051017
16. Belforte P, Cheli F, Diana G, Melzi S (2008) Numerical and experimental approach for the evaluation of severe longitudinal dynamics of heavy freight trains. Veh Syst Dyn 46(sup1):937–955
17. UIC (2004) 544-1: brakes—braking power
18. Di Gialleonardo E, Melzi S, Trevisi D (2022) Freight trains for intermodal transportation: optimisation of payload distribution for reducing longitudinal coupling forces. Veh Syst Dyn. https://doi.org/10.1080/00423114.2022.2120025
19. Bosso N, Magelli M, Rossi Bartoli L, Zampieri N (2022) The influence of resistant force equations and coupling system on long train dynamics simulations. Proc Inst Mech Eng Part F J Rail Rapid Transit 236(1):35–47
20. Zhang Z, Li G, Chu G, Zu H, Kennedy D (2015) Compressed stability analysis of the coupler and buffer system of heavy-haul locomotives. Veh Syst Dyn 53(6):833–855
21. UIC (2006) 540: brakes—air brakes for freight trains and passenger trains
22. Bosso N, Gugliotta A, Magelli M, Oresta IF, Zampieri N (2019) Study of wheel-rail adhesion during braking maneuvers. Procedia Struct Integr 24:680–691
23. Pugi L, Rindi A, Ercole AG, Palazzolo A, Auciello J, Fioravanti D, Ignesti M (2011) Preliminary studies concerning the application of different braking arrangements on Italian freight trains. Veh Syst Dyn 49(8):1339–1365
24. Pugi L, Malvezzi M, Allotta B, Banchi L, Presciani P (2004) A parametric library for the simulation of a Union Internationale des Chemins de Fer (UIC) pneumatic braking system. Proc Inst Mech Eng Part F J Rail Rapid Transit 218(2):117–132